

# Reduced dynamics with renormalization in solid-state charge qubit measurement

JunYan Luo,<sup>1,\*</sup> Hujun Jiao,<sup>2</sup> Feng Li,<sup>2</sup> Xin-Qi Li,<sup>1,2,3</sup> and YiJing Yan<sup>1</sup>

*<sup>1</sup>Department of Chemistry, Hong Kong University  
of Science and Technology, Kowloon, Hong Kong*

*<sup>2</sup>State Key Laboratory for Superlattices and Microstructures,  
Institute of Semiconductors, Chinese Academy of Sciences,  
P.O. Box 912, Beijing 100083, China*

*<sup>3</sup>Department of Physics, Beijing Normal University, Beijing 100875, China*

## Abstract

Quantum measurement will inevitably cause backaction on the measured system, resulting in the well known dephasing and relaxation. In this report, in the context of solid-state qubit measurement by a mesoscopic detector, we show that an alternative backaction known as *renormalization* is important under some circumstances. This effect is largely overlooked in the theory of quantum measurement.

PACS numbers: 03.65.Ta, 03.67.Lx, 73.23.-b, 85.35.Be

---

\*Electronic address: firstluo@semi.ac.cn

## I. INTRODUCTION

One of the key requirements for physically implementing quantum computation is the ability to readout a two-state quantum system (qubit). Among various proposals, an important one is to use an electrometer as detector whose conductance depends on the charge state of a nearby qubit. Such electrometer can be a quantum point contact (QPC) [1, 2, 3, 4, 5, 6, 7, 8], or a single electron transistor [9, 10, 11, 12, 13, 14, 15, 16]. Both of them have been preliminarily implemented in experiment for quantum measurements [17, 18, 19, 20, 21]. Also, similar structures were proposed for entanglement generation and detection by conduction electrons [22, 23, 24].

The problem of measuring a charge qubit by a QPC detector has been well studied in high bias voltage regime. Work for arbitrary measurement voltage has also been reported although relatively limited [8, 25]. Most of them only dealt with the measurement induced dephasing and relaxation, which, from the perspective of information, are consequences of information acquisition by measurement. The physical interaction between the measurement apparatus and the qubit, however, give rise to another important backaction which renormalizes the internal structure of qubit.

In this context, we revisit the measurement problem, while take fully into account of the energy renormalization. This effect was often disregarded in the literature. Indeed, the steady-state renormalization can be effectively included in the Caldeira–Leggett renormalized system Hamiltonian [26, 27, 28, 29]. The resulting dynamics is however different in detail from that of the dynamical renormalization approach [26, 27]. The apparent distinction should be sensitively reflected in the output power spectral density studied in this work. Our analysis shows that the renormalization effect on qubit becomes increasingly important as one lowers the measurement voltage. Therefore, it would require in practice to have this feature being taken into account properly, in order to correctly analyze and understand the measurement results.

## II. MODEL DESCRIPTION

The system under investigation is schematically shown in Fig. 1. The Hamiltonian of the entire system is of  $H_T = H_{\text{qu}} + H_D + H'$ , with the qubit, QPC detector, and their coupling

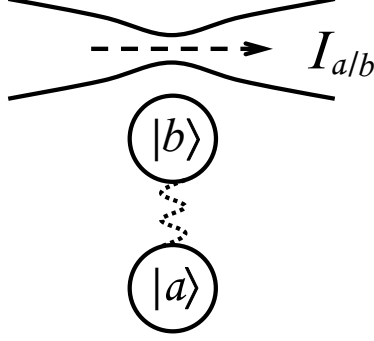


FIG. 1: Schematic setup of a solid–state charge qubit measured continuously by a quantum–point–contact (QPC).

parts being modeled respectively by

$$H_{\text{qu}} = \sum_{s=a,b} \epsilon_s |s\rangle\langle s| + \frac{1}{2} \Delta (|a\rangle\langle b| + |b\rangle\langle a|), \quad (1a)$$

$$H_{\text{D}} = \sum_{k \in \text{L}} \epsilon_k \hat{c}_k^\dagger \hat{c}_k + \sum_{q \in \text{R}} \epsilon_q \hat{c}_q^\dagger \hat{c}_q, \quad (1b)$$

$$H' = \sum_{s=a,b} \sum_{k,q} t_{kq}^s \hat{c}_k^\dagger \hat{c}_q \cdot |s\rangle\langle s| + \text{H.c.} \quad (1c)$$

The amplitude  $t_{kq}^s$  of electron tunneling through two reservoirs ( $\alpha = \text{L}$  and  $\text{R}$ ) of the QPC depends explicitly on the qubit state. Denote  $Q_s \equiv |s\rangle\langle s|$  hereafter. Thus, the qubit–QPC detector coupling reads in the  $H_{\text{D}}$ –interaction picture as  $H'(t) = \sum_s [\hat{f}_s(t) + \hat{f}_s^\dagger(t)] \cdot Q_s$ , with  $\hat{f}_s(t) \equiv e^{iH_{\text{D}}t} (\sum_{kq} t_{kq}^s \hat{c}_k^\dagger \hat{c}_q) e^{-iH_{\text{D}}t}$ . The effects of the stochastic QPC reservoirs on measurement are characterized by  $\tilde{C}_{ss'}^{(+)}(t-\tau) \equiv \langle \hat{f}_s^\dagger(t) \hat{f}_{s'}(\tau) \rangle$  and  $\tilde{C}_{ss'}^{(-)}(t-\tau) \equiv \langle \hat{f}_s(t) \hat{f}_{s'}^\dagger(\tau) \rangle$ . In terms of the reservoirs spectral density functions, which are defined physically as

$$J_{ss'}(\omega, \omega') = \sum_{k,q} t_{kq}^s t_{kq}^{s'} \delta(\omega - \epsilon_k) \delta(\omega' - \epsilon_q), \quad (2)$$

these QPC coupling correlation functions are

$$\tilde{C}_{ss'}^{(\pm)}(t) = \iint d\omega d\omega' J_{ss'}(\omega, \omega') f_{\text{L}}^{(\pm)}(\omega) f_{\text{R}}^{(\mp)}(\omega') e^{i(\omega - \omega')t}.$$

Here,  $f_{\alpha}^{(\pm)}(\omega) = \{1 + e^{\pm\beta(\omega - \mu_{\alpha})}\}^{-1}$  relates to the Fermi function of the lead  $\alpha$ , with  $\beta = (k_{\text{B}}T)^{-1}$  the inverse temperature. The coupling spectrum function used later is defined by

$$C_{ss'}^{(\pm)}(\omega) \equiv \int_{-\infty}^{\infty} dt \tilde{C}_{ss'}^{(\pm)}(t) e^{-i\omega t}. \quad (3)$$

Throughout this work, we set  $\mu_L^{\text{eq}} = \mu_R^{\text{eq}} = 0$  for the equilibrium chemical potentials (or Fermi energies) of the QPC reservoirs in the absence of applied bias voltage, and  $\hbar = e = 1$  for the Planck constant and electron charge.

### III. PARTICLE-NUMBER-RESOLVED MASTER EQUATION

The reduced density matrix of the qubit is formally defined as  $\rho(t) \equiv \text{Tr}_D[\rho_T(t)]$ , i.e., tracing out the QPC reservoirs degree of freedom over the entire qubit-plus-detector density matrix. The qubit system Liouvillian is defined via  $\mathcal{L}\hat{O} \equiv [H_{\text{qu}}, \hat{O}]$ . By treating  $H'$  as perturbation, a master equation for the reduced density matrix can be derived as [26, 27, 30]

$$\dot{\rho}(t) = -i\mathcal{L}\rho(t) - \frac{1}{2} \sum_s [Q_s, \tilde{Q}_s \rho(t) - \rho(t) \tilde{Q}_s^\dagger], \quad (4)$$

with  $\tilde{Q}_s \equiv \tilde{Q}_s^{(+)} + \tilde{Q}_s^{(-)}$ , and

$$\tilde{Q}_s^{(\pm)} \equiv \sum_{s'} [C_{ss'}^{(\pm)}(\mathcal{L}) + iD_{ss'}^{(\pm)}(\mathcal{L})] Q_{s'}. \quad (5)$$

Here,  $C_{ss'}^{(\pm)}(\mathcal{L}) \equiv C_{ss'}^{(\pm)}(\omega)|_{\omega=\mathcal{L}}$  is the spectrum function defined earlier. The dispersion function  $D_{ss'}^{(\pm)}(\mathcal{L})$  can then be evaluated via the Kramers-Kronig relation,

$$D_{ss'}^{(\pm)}(\omega) = \frac{1}{\pi} \mathcal{P} \int_{-\infty}^{\infty} d\omega' \frac{C_{ss'}^{(\pm)}(\omega')}{\omega - \omega'}. \quad (6)$$

Physically, it is responsible for the renormalization [26, 27, 28, 29].

To achieve a description of the output from detector, we employ the transport particle number “ $n$ ”-resolved reduced density matrices  $\{\rho^{(n)}(t); n = 0, 1, \dots\}$  that satisfy  $\rho(t) = \sum_n \rho^{(n)}(t)$ . The corresponding “ $n$ ”-resolved conditional quantum master equation reads [8, 31, 32]

$$\begin{aligned} \dot{\rho}^{(n)}(t) = & -i\mathcal{L}\rho^{(n)}(t) - \frac{1}{2} \sum_s \{ Q_s \tilde{Q}_s \rho^{(n)} - \tilde{Q}_s^{(-)} \rho^{(n-1)} Q_s \\ & - \tilde{Q}_s^{(+)} \rho^{(n+1)} Q_s + \text{H.c.} \}. \end{aligned} \quad (7)$$

We would like to account for the finite bandwidth of the QPC detector, which will be characterized by a single Lorentzian. Real spectral density has a complicated structure, which can be parameterized via the technique of spectral decomposition [33, 34]. This complexity, however, will only modify details of the results, but not the qualitative picture.

For the sake of constructing analytical results, we assume a simple Lorentzian function centered at the Fermi energy for the spectral density Eq. (2). This choice stems also from the assumption that the energy band of each reservoir is half-filled. Moreover, the bias voltage is conventionally described by a relative shift of the entire energy-bands, thus the centers of the Lorentzian functions would fix at the Fermi levels. Without loss of generality, we simply assume

$$J_{ss'}(\omega, \omega') = \mathcal{T}_s \mathcal{T}_{s'} \frac{\Gamma_L^0 w^2}{(\omega - \mu_L)^2 + w^2} \cdot \frac{\Gamma_R^0 w^2}{(\omega' - \mu_R)^2 + w^2}. \quad (8)$$

We set  $\mathcal{T}_a \equiv 1$  and  $\mathcal{T}_b \equiv 1 - \chi$ . The asymmetric qubit-QPC coupling parameter is of  $0 < \chi < 1$ , as inferred from Fig. 1. The correlation function of Eq. (3) can be evaluated as  $C_{ss'}^{(\pm)}(\omega) = \mathcal{T}_s \mathcal{T}_{s'} C^{(\pm)}(\omega)$ , with

$$C^{(\pm)}(\omega) = \frac{\eta g(x)}{1 - e^{\beta x}} \left[ \frac{w^2}{x} \{ \phi(0) - \phi(x) \} - \frac{w}{2} \varphi(x) \right]_{x=\omega \pm V}. \quad (9)$$

Here,  $\eta = 2\pi\Gamma_L^0\Gamma_R^0$ ,  $g(x) = 4w^2/(x^2 + 4w^2)$ , and  $V = \mu_L - \mu_R$  the applied voltage on the QPC detector;  $\phi(x)$  and  $\varphi(x)$  denote the real and imaginary parts of the digamma function  $\Psi(\frac{1}{2} + \beta\frac{w+ix}{2\pi})$ , respectively. Knowing the spectral function, the dispersion function  $D_{ss'}^{(\pm)}(\omega) = \mathcal{T}_s \mathcal{T}_{s'} D^{(\pm)}(\omega)$  can be obtained via the Kramers-Kronig relation. The present spectrum functions satisfy the detailed-balance relation  $C^{(+)}(\omega) = e^{-\beta(\omega+V)} C^{(-)}(-\omega)$ . This means that our approach properly accounts for the energy exchange between the qubit and the detector during measurement.

#### IV. OUTPUT POWER SPECTRAL DENSITY

In continuous weak measurement of qubit oscillations, the most important output is the spectral density of current. Typically, the power spectrum is defined with a stationary state. The involving stationary-state  $\rho^{\text{st}}$  can be determined by setting  $\dot{\rho}^{\text{st}} = 0$  in Eq. (4), together with the normalization condition, at given bias voltage and temperature. For clarity, we focus hereafter on the symmetric qubit case, with the state energies of  $\epsilon_a = \epsilon_b = 0$ .

Let us start with the average current. Using the “ $n$ ”-resolved master equation (7), the average current can be expressed as  $I(t) = \sum_n n \text{Tr}[\dot{\rho}^{(n)}(t)] = \text{Tr}[\mathcal{J}^{(-)}\rho(t)]$ , where  $\mathcal{J}^{(-)}$  is one of the superoperators, defined as

$$\mathcal{J}^{(\pm)}\rho(t) \equiv \frac{1}{2} \sum_s (\tilde{Q}_s^{(-)} \pm \tilde{Q}_s^{(+)}) \rho(t) Q_s + \text{H.c.} \quad (10)$$

The stationary current can be carried out as

$$\bar{I} = I_a \rho_{aa}^{\text{st}} + I_b \rho_{bb}^{\text{st}} + I_{ab} \rho_{ab}^{\text{st}}, \quad (11)$$

which for a symmetric qubit ( $\epsilon_a = \epsilon_b = 0$ ) is of

$$\begin{aligned} I_a &= \left(1 - \frac{\chi}{2}\right) C(0) \tanh\left(\frac{\beta V}{2}\right) + \chi \bar{\gamma}_+, \\ I_b &= (1 - \chi) \left[ \left(1 - \frac{\chi}{2}\right) C(0) \tanh\left(\frac{\beta V}{2}\right) - \chi \bar{\gamma}_+ \right], \\ I_{ab} &= \chi^2 \bar{\gamma}_-. \end{aligned} \quad (12)$$

Here,  $\bar{\gamma}_{\pm} \equiv \frac{1}{4} [\bar{C}(\Delta) \pm \bar{C}(-\Delta)]$ , with  $\bar{C}(\omega) \equiv C^{(-)}(\omega) - C^{(+)}(\omega)$ . Denote also  $C(\omega) \equiv C^{(-)}(\omega) + C^{(+)}(\omega)$ .

The noise spectral density can be calculated via the MacDonald's formula [35]

$$S(\omega) = 2\omega \int_0^{\infty} dt \sin(\omega t) \frac{d}{dt} [\langle n^2(t) \rangle - (\bar{I}t)^2], \quad (13)$$

with  $\langle n^2(t) \rangle \equiv \sum_n n^2 \text{Tr}\{\rho^{(n)}(t)\}$ . Applying equation (7) gives

$$\frac{d}{dt} \langle n^2(t) \rangle = \text{Tr}[2\mathcal{J}^{(-)}N(t) + \mathcal{J}^{(+)}\rho^{\text{st}}], \quad (14)$$

where  $N(t) \equiv \sum_n n \rho^{(n)}(t)$ , which can be calculated via

$$\frac{dN}{dt} = -i\mathcal{L}N - \frac{1}{2} \sum_s [Q_s, \tilde{Q}_s N - N \tilde{Q}_s^\dagger] + \mathcal{J}^{(-)}\rho(t). \quad (15)$$

For a symmetric qubit, analytical result is available. We split the spectrum into four components,  $S = S_0 + S_1 + S_2 + S_3$ , and present them one-by-one as follows. First, the frequency-independent background noise  $S_0$  reads

$$\begin{aligned} S_0 &= 2\bar{I} \coth\left(\frac{\beta V}{2}\right) - \chi^2 (\gamma_- / \gamma_+) [\gamma_- - \bar{\gamma}_- \coth\left(\frac{\beta V}{2}\right)] \\ &\quad + \chi [\chi - (2 - \chi) \delta \bar{P}] [\gamma_+ - \bar{\gamma}_+ \coth\left(\frac{\beta V}{2}\right)], \end{aligned} \quad (16)$$

with  $\gamma_{\pm} \equiv \frac{1}{4} [C(\Delta) \pm C(-\Delta)]$  and  $\delta \bar{P} \equiv \rho_{bb}^{\text{st}} - \rho_{aa}^{\text{st}}$  that is nonzero due to the asymmetric qubit-QPC coupling. The second component is a Lorentzian, with the peak at  $\omega = 0$  and the dephasing rate of  $\gamma_d = \chi^2 \gamma_+$ . It reads

$$S_1 = (X\gamma_d - \chi^2 \gamma_- \bar{I}) \frac{2I_{ab}}{\omega^2 + \gamma_d^2}. \quad (17)$$

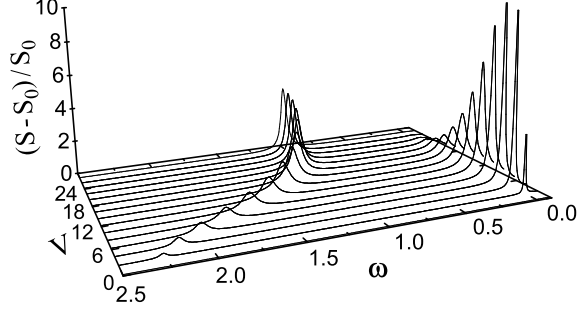


FIG. 2: Power spectral density of the detector current, with the frequency and voltage labeled in unit of  $\Delta$ . The bandwidth  $w = 15\Delta$ . Other parameters are  $\eta = 2$ ,  $\chi = 0.2$  and  $\beta\Delta = 1$ .

Here,  $2\langle a|\mathcal{J}^{(+)}\rho^{\text{st}}|b\rangle \equiv X + iY$  (the real and imaginary parts). We remark that  $S_1$  arises completely from the qubit relaxation induced inelastic tunneling effect in the detector[8]. The last two components are

$$S_2 = \left[ \frac{(\chi^2\gamma_- \bar{I} - X\gamma_d)\tilde{\epsilon}}{\omega^2 + \gamma_d^2} + Y \right] \frac{\omega^2\gamma'_d A - (\omega\omega' - \Delta\tilde{\Delta})B}{\omega^2\gamma'^2_d + (\omega\omega' - \Delta\tilde{\Delta})^2}, \quad (18)$$

$$S_3 = \left[ \frac{(\chi^2\gamma_- \bar{I}\gamma_d + X\omega^2)\tilde{\epsilon}}{\omega^2 + \gamma_d^2} - \Delta Z \right] \frac{\gamma'_d B - (\omega\omega' - \Delta\tilde{\Delta})A}{\omega^2\gamma'^2_d + (\omega\omega' - \Delta\tilde{\Delta})^2}. \quad (19)$$

Here,  $\tilde{\epsilon}$  and  $\tilde{\Delta}$  are the renormalized version of the original  $\epsilon \equiv \epsilon_a - \epsilon_b$  and  $\Delta$  of the qubit. They are related to the dispersion functions of the detector. Let  $D(\omega) \equiv D^{(-)}(\omega) + D^{(+)}(\omega)$  and  $\bar{D}(\omega) \equiv D^{(-)}(\omega) - D^{(+)}(\omega)$ . Simple analysis on the symmetric case ( $\epsilon = 0$ ) gives

$$\tilde{\epsilon} = \chi\left(1 - \frac{\chi}{2}\right)D(0), \quad (20a)$$

$$\tilde{\Delta} = \Delta + \frac{1}{4}\chi^2[D(\Delta) - D(-\Delta)]. \quad (20b)$$

For the bookkeeping of Eqs. (18) and (19), we have also introduced  $Z \equiv \frac{1}{2}[(I_a + I_b)\delta\bar{P} + (I_a - I_b)] + (\frac{2}{\chi} - 1)I_{ab}\rho_{ab}^{\text{st}}$ , and the frequency-dependent quantities of

$$\begin{aligned} \omega' &\equiv \omega\left(1 - \frac{\tilde{\epsilon}^2}{\omega^2 + \gamma_d^2}\right), & \gamma'_d &\equiv \gamma_d\left(1 + \frac{\tilde{\epsilon}^2}{\omega^2 + \gamma_d^2}\right), \\ A &\equiv \chi\left(1 - \frac{\chi}{2}\right)[\bar{D}(\Delta) - \bar{D}(-\Delta)] + 2\tilde{\epsilon}I_{ab}\frac{\gamma_d^2}{\omega^2 + \gamma_d^2}, \\ B &\equiv -2(I_a - I_b)\Delta + 2\tilde{\epsilon}I_{ab}\frac{\omega^2}{\omega^2 + \gamma_d^2}. \end{aligned} \quad (21)$$

The computed noise spectrum is displayed in Fig. 2. It is of interest to note that the spectral peak apart from the zero frequency, which is the signal of qubit oscillations, shifts

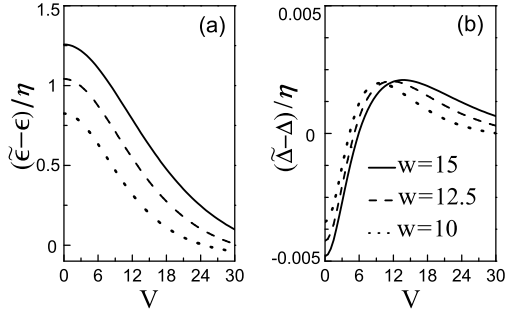


FIG. 3: Renormalization on the qubit level energy (a) and coupling (b), exemplified with three values of bandwidth  $w$  (in unit of  $\Delta$ ). Other parameters are the same as in Fig. 2.

with the measurement voltages. (i) In the high voltage regime (e.g. for  $V \gtrsim 30 \Delta$  as shown in Fig. 2), the oscillation peak locates approximately at  $\omega \approx \Delta$ ; (ii) As lowering the voltage, the measurement induced renormalization effect becomes increasingly important, which strongly affects the position of the oscillation peak.

The feature of the noise spectrum in Fig. 2 is closely related to the renormalization of the qubit parameters  $\epsilon$  and  $\Delta$ . In the limit of weak qubit-QPC coupling, the renormalized Rabi frequency is given by  $\omega_R = \sqrt{\tilde{\epsilon}^2 + \tilde{\Delta}^2}$ . The renormalization effect  $(\omega_R - \sqrt{\epsilon^2 + \Delta^2})$  increases *monotonically* with the QPC bandwidth ( $w$ ). In Fig. 3 we plot  $\tilde{\epsilon}$  and  $\tilde{\Delta}$ , in terms of the  $\eta$ -scaled renormalizations, against the bias voltage for different bandwidths. The renormalized qubit state energy difference  $\tilde{\epsilon}$  increasingly deviates from the original  $\epsilon = 0$  as the QPC bandwidth increases or the applied voltage decreases, as shown in Fig. 3(a). In contrast, the inter-state coupling renormalization is negligibly small, as depicted in Fig. 3(b) and also claimed in Ref. [25]. That  $(\tilde{\epsilon} - \epsilon)$  being dominant can be readily understood by the form of coupling  $H'$  of Eq. (1c), which modulates the level energies, rather than the level coupling. In the wideband limit ( $w \rightarrow \infty$ ), the energy renormalization would diverge. However, this feature is an artifact, since in reality a natural cutoff of the bandwidth must exist. That's the reason we introduce a Lorentzian cut-off in Eq. (8).

The noise spectrum itself depends on  $\eta$  in a rather complicated manner, especially the  $S_2$  and  $S_3$  components [Eq. (18) or Eq. (19) with Eq. (21)] that are of dynamical in nature. In contrast, the algebraic nonlinear dependence of  $\eta$  in the average current  $\bar{I}$  Eq. (11) and  $S_0$  Eq. (16) arises from the renormalized stationary  $\rho^{\text{st}}$  only. In literature (e.g. Ref. [25])

the dispersion function is often disregarded explicitly, with its effect being included in the Caldeira-Leggett renormalized system Hamiltonian[26, 27, 28, 29]. However, this approach gives rise to quite different dynamics from the present result, even though their stationary state behaviors could be similar [26, 27]. Apparently, the dynamical distinct should be sensitively reflected in the shot noise spectrum. In the context of qubit measurement by a QPC detector, our analysis can be served as a detailed investigation of the dynamical renormalization effect.

In Fig. 4 we further show the signal-to-noise ratio of the noise spectrum against the bias voltage for different bandwidths. In the limit of large bias  $V \gg \Delta$  and for weak qubit-QPC coupling, the signal-to-noise ratio

$$\left. \frac{S(\omega_R) - S_0}{S_0} \right|_{V \gg \Delta} \rightarrow 4 \frac{(2 - \chi)^2}{(2 - \chi)^2 + \chi^2} \quad (22)$$

can reach the limit of 4; i.e. the Korotkov-Averin bound for any linear response detectors [3, 36, 37, 38].

As seen in Fig. 2, the detector induced renormalization also results in a wide voltage range where the coherent peak at the renormalized Rabi frequency and the sharp peak at zero frequency coexist. In that regime, the level mismatch induced by the detector is prominent, while the qubit coherence is not strongly destroyed. As is well known [3, 25, 39], the peak at zero frequency is a signature of the Zeno effect in continuous weak measurement. The basic picture is that the detector attempts to localize the electron in one of the levels for a longer time, leading thus to incoherent jumps between the two levels. Finally, in Fig. 2, the coherent peak persists to high bias voltage, while the zero-frequency peak eventually disappears. This feature is different from the previous work [8]. The reason is twofold. On one hand, as shown in Fig. 3, the renormalization of energy levels is weak at high voltage. On the other hand, in this work we adopted a finite bandwidth model for the QPC. This implies that in high voltage regime the QPC (measurement) current is weak, which differs from the result under the usual wide-band approximation. As a consequence, the weak backaction from the detector together with the alignment of the qubit levels results in the spectral feature shown in Fig. 2 at high voltages.

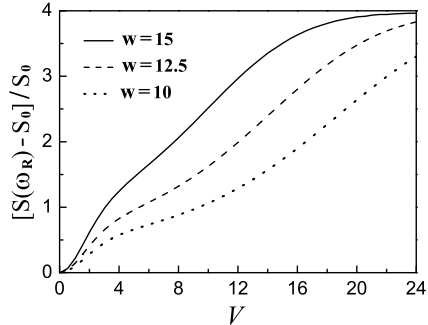


FIG. 4: Bias voltage dependence of the peak-to-pedestal ratio of the output power spectrum, exemplified with the same parameters in Fig. 3.

## V. CONCLUSIONS

In summary, we have revisited the problem of continuous measurement of a solid-state qubit by quantum point contact. Our results showed that the renormalization effect, which was neglected in previous studies, can significantly affect the output power spectrum. This feature should be taken into account in the interpretation of measurement result. We also note that the renormalization in the present setup may be quantified *in situ*. No reference to the bare qubit is needed, as it can be effectively replaced the band-edge large voltage transport limit.

### Acknowledgments

This work is supported by RGC (604007 & 604508) of Hong Kong SAR Government, the National Natural Science Foundation (60425412 & 90503013), and Major State Basic Research Project (2006CB921201) of China.

- 
- [1] I. L. Aleiner, N. S. Wingreen, and Y. Meir, Phys. Rev. Lett. **79**, 3740 (1997).
  - [2] S. A. Gurvitz, Phys. Rev. B **56**, 15215 (1997).
  - [3] A. N. Korotkov and D. V. Averin, Phys. Rev. B **64**, 165310 (2001).
  - [4] H. S. Goan, G. J. Milburn, H. M. Wiseman, and H. B. Sun, Phys. Rev. B **63**, 125326 (2001).
  - [5] D. V. Averin and E. V. Sukhorukov, Phys. Rev. Lett. **95**, 126803 (2005).

- [6] S. Pilgram and M. Büttiker, *Phys. Rev. Lett.* **89**, 200401 (2002).
- [7] A. A. Clerk, S. M. Girvin, and A. D. Stone, *Phys. Rev. B* **67**, 165324 (2003).
- [8] X. Q. Li, P. Cui, and Y. J. Yan, *Phys. Rev. Lett.* **94**, 066803 (2005).
- [9] A. Shnirman and G. Schön, *Phys. Rev. B* **57**, 15400 (1998).
- [10] M. H. Devroret and R. J. Schoelkopf, *Nature* **406**, 1039 (2000).
- [11] Y. Makhlin, G. Schön, and A. Shnirman, *Rev. Mod. Phys.* **73**, 357 (2001).
- [12] A. A. Clerk, S. M. Girvin, A. K. Nguyen, and A. D. Stone, *Phys. Rev. Lett.* **89**, 176804 (2002).
- [13] H. Jiao, X.-Q. Li, and J. Y. Luo, *Phys. Rev. B* **75**, 155333 (2007).
- [14] T. Gilad and S. A. Gurvitz, *Phys. Rev. Lett.* **97**, 116806 (2006).
- [15] S. A. Gurvitz and G. P. Berman, *Phys. Rev. B* **72**, 073303 (2005).
- [16] N. P. Oxtoby, H. M. Wiseman, and H.-B. Sun, *Phys. Rev. B* **74**, 045328 (2006).
- [17] E. Buks, R. Schuster, M. Heiblum, D. Mahalu, and V. Umansky, *Nature* **391**, 871 (1998).
- [18] R. J. Schoelkopf, P. Wahlgren, A. A. Kozhevnikov, P. Delsing, and D. E. Prober, *Science* **280**, 1238 (1998).
- [19] Y. Nakamura, Y. A. Pashkin, and J. S. Tsai, *Nature (London)* **398**, 786 (1999).
- [20] D. Sprinzak, E. Buks, M. Heiblum, and H. Shtrikman, *Phys. Rev. Lett.* **84**, 5820 (2000).
- [21] A. Aassime, G. Johansson, G. Wendin, R. J. Schoelkopf, and P. Delsing, *Phys. Rev. Lett.* **86**, 3376 (2001).
- [22] J. M. Elzerman, R. Hanson, L. H. W. van Beveren, B. Witkamp, L. M. K. Vandersypen, and L. P. Kouwenhoven, *Nature* **430**, 431 (2004).
- [23] B. Trauzettel, A. N. Jordan, C. W. J. Beenakker, and M. Büttiker, *Phys. Rev. B* **73**, 235331 (2006).
- [24] H. Schomerus and J. P. Robinson, *New J. Phys.* **9**, 67 (2007).
- [25] A. Shnirman, D. Mozyrsky, and I. Martin, LANL e-print cond-mat/0211618 (2002).
- [26] R. X. Xu and Y. J. Yan, *J. Chem. Phys.* **116**, 9196 (2002).
- [27] Y. J. Yan and R. X. Xu, *Annu. Rev. Phys. Chem.* **56**, 187 (2005).
- [28] A. O. Caldeira and A. J. Leggett, *Physica A* **121**, 587 (1983).
- [29] U. Weiss, *Quantum Dissipative Systems* (World Scientific, Singapore, 2008), 3rd ed.
- [30] Y. J. Yan, *Phys. Rev. A* **58**, 2721 (1998).
- [31] X. Q. Li, J. Y. Luo, Y. G. Yang, P. Cui, and Y. J. Yan, *Phys. Rev. B* **71**, 205304 (2005).
- [32] J. Y. Luo, X.-Q. Li, and Y. J. Yan, *Phys. Rev. B* **76**, 085325 (2007).

- [33] C. Meier and D. J. Tannor, *J. Chem. Phys.* **111**, 3365 (1999).
- [34] X. Q. Li and Y. J. Yan, *Phys. Rev. B* **75**, 075114 (2007).
- [35] D. K. C. MacDonald, *Noise and Fluctuations: An Introduction* (Wiley, New York, 1962), ch. 2.2.1.
- [36] A. N. Korotkov, *Phys. Rev. B* **63**, 085312 (2001).
- [37] D. V. Averin and A. N. Korotkov, *Phys. Rev. Lett.* **94**, 069701 (2005).
- [38] H. Jiao, S.-K. Wang, F. Li, and X.-Q. Li, arXiv:0806.2502 (2008).
- [39] S. A. Gurvitz, L. Fedichkin, D. Mozyrsky, and G. P. Berman, *Phys. Rev. Lett.* **91**, 066801 (2003).